ELSEVIER

Biophysical Chemistry 49 (1994) 201–214

Biophysical Chemistry

Monte Carlo simulations on potentiometric titration of cylindrical polyelectrolytes: Introduction of a method and its application to model systems without added salt

Takuhiro Nishio

Department of Physics, Hamamatsu University School of Medicine, Hamamatsu 431-31, Japan

(Received 21 June 1993; accepted 6 September 1993)

Abstract

A novel method of the Monte Carlo simulation on the potentiometric titration behavior is developed for an aqueous salt-free solution of rod-like polyelectrolytes in a cylindrical cell system. The trials are attempted in an iterative loop for the ionization and deionization of each ionizable group on the polymer rod as well as for the random motion of small ions within the cell free volume by using the Monte Carlo criterion. In the simulation, pH value of the aqueous solution is assumed as a fixed parameter that determines the excess energy with ionization process. The interaction between charged species is modeled as a combination of a point charge on an impenetrable rod surface and a charged hard sphere with several sizes. The averaged degree of ionization, the ion distribution around the polyion and other thermodynamic quantities are finally obtained as those of the equilibrium state by repeating iteration after the convergence is fulfilled. The results are compared with the analytical solutions of the Poisson–Boltzmann (PB) equation for the uniformly charged cylindrical polyelectrolytes. The counterion distribution agrees with each other, whereas the titration curve is deviated from the PB results. The deviation is interpreted as the difference in the electrostatic free energies between both models. The characteristics as well as the limitations of the present method are also discussed.

Key words: Potentiometric titration; Polyelectrolyte; Cylindrical cell model; Monte Carlo simulation; Counterion distribution; Electrostatic free energy

1. Introduction

On the theoretical studies of the polyelectrolyte solution, the rod-like polyelectrolyte models frequently adopted are classified into two types according to the charge distribution on the polymer skeleton. One is the uniformly charged model, and the other is the discrete site model.

The uniformly charged assumption had been introduced because of its facility in the calculation of the electrostatic potential and the related quantities of the cylindrical polyion-small ion system. One of the most useful methods is the solution of the Poisson–Boltzmann (PB) equation to calculate the electrostatic energy as well as the ionic distribution in the uniformly charged model system. The quantitative interpretations of the titration curves of various polyelectrolytes and proteins have been achieved by the method of the PB equation [1–4]. In the treatment, the charac-

SSDI 0301-4622(93)E0070-L

teristics of the polyion species are reduced, that is, the arrangement of the charged groups on the polymer is expressed by a few parameters, such as its radius and the mean charge density. In addition, it is often necessary that the unreasonable molecular dimension is introduced as an adjustable parameter for curve fitting to the experimental data.

Manning's counterion condensation (CC) hypothesis, which is another influential theory, has revealed many critical features of the polyelectrolyte solution. In its application to the potentiometric titration, the singular point, which has never been observed experimentally, appears on the titration curve at a critical value of polyion charge density [5]. Owing to these difficulties, it seems to be another problem that the free energy of the system has to be calculated at a fixed degree of ionization in the uniformly charged model. A measurable degree of ionization intrinsically must be an averaged value of many dispersed states.

In the discrete site model, the arrangement of the ionizable group can be treated in detail, and the physical quantities are calculated by the techniques developed in the statistical physics. The partition function of the system in the titration process is obtained using matrix methods [6–8]. Other techniques are also available to evaluate the averaged quantities [9–11]. The characteristics of various titration curves are well represented qualitatively as the results of the numerical computations. Two-step dissociation observed in the polymer of maleic acid is interpreted solely by this model. It is necessary, however, to remark that the interaction between the charged species is oversimplified in the model. Since a simple function, for example the Debye–Hückel (DH) type, and its additivity for the electrostatic potential are postulated as the interaction between the charged groups, the nonlinear effect of the mobile ion accumulation around the polyion is so difficult to be considered in the model. The ionic strength in the solution sometimes has to be treated as a tentative parameter for fitting to the experimental data [12].

Taking account of the characteristics and difficulties of both charged models, the Monte Carlo (MC) study on the discrete site model seems to be a more hopeful method to simulate the titration behavior. In the recent decade, the MC simulation becomes a powerful method for the many-body problem by the development of various techniques [13]. Numerous MC studies have been carried out for the ionic distribution around a rod-like polyelectrolyte (particularly, for the DNA molecule) in a cylindrical cell system and many interesting properties of the polyelectrolyte solutions were revealed [14–21]. It is expected that the several difficulties of the theoretical approach can be overcome by the MC simulation on the potentiometric titration.

In the present paper, a new canonical MC simulation technique is presented for the potentiometric titration of a salt-free solution of rod-like polyelectrolytes as a function of pH. Ionization and deionization processes accompanied by the insertion and deletion of a counterion modeled as a charged hard sphere, as well as the movement of small ions are simulated in the cylindrical cell system using the MC sampling algorithm. After the convergence of the state is achieved, several quantities of the system, summed up in the iterative loop are calculated as those of the equilibrium state. The degree of ionization, the small ion distribution around the polyion, the enthalpy and entropy part of the electrostatic free energies of the whole system and other quantities are obtained as a function of pH. The effect of the group arrangement of ionizable groups on the polymer rod is also tested in this system. The titration curves are found to be deviated from those obtained by the analytical solutions of the PB equation, due to the energetic difference, revealed by the comparison of the free energies in both systems. The restrictions of the model (especially, about the treatment of solution pH) are also discussed as the problems of the polyelectrolyte theory.

2. Model and method

2.1. Cylindrical cell model

In the simulation, a well-known cylindrical cell model is adopted as an isolated polyelectrolyte

system with mobile small ions. The cylindrical space with its height, H, and the radius, R, is assumed to be a central objective cell. An impenetrable thin rod, whose radius is a, with N_p helically arranged ionizable groups is centered in the objective cell as a polymer cylinder. The mean axial distance per fixed group is denoted by b, and ξ^{max} is the linear charge density parameter at the fully ionized state. The relations among these parameters and the concentration of the ionizable groups, C_p, are given, as follows:

$$b = H/N_p \tag{1}$$

$$\xi^{max} = e^2/(4\pi\epsilon_0 D b k_B T) \tag{2}$$

$$C_p = \frac{1}{N_{AV}} \frac{N_p}{\pi R^2 H} \tag{3}$$

where e is the elementary protonic charge, ϵ_0, the permittivity of the vacuum, D, the relative dielectric constant of the solvent, k_B, the Boltzmann constant, T, the absolute temperature, and N_{AV}, Avogadro's constant. To calculate the external potential, the central objective cell is placed between two sufficiently long external cells whose resultant length is $2L$. The external cells consist of the smeared charge distribution equivalent to that of the central cell to satisfy the boundary condition.

Each neutral ionizable group can be dissociated into an ionized group with charge $-e$, and a mobile monovalent counterion with charge $+e$ and radius σ_m. An ionizable group is assumed to be dimensionless ($\sigma_p = 0$), that is, buried in the polymer rod surface. When N_m ($\leqslant N_p$) ionizable groups are dissociated and the same number of the counterions are released into the cell, the degree of ionization, α, the mean charge density parameter, ξ, and the mean counterion concentration in the cell free volume, C_m^{mean}, are defined as,

$$\alpha = N_m/N_p \tag{4}$$

$$\xi = \alpha\xi^{max} \tag{5}$$

$$C_m^{mean} = \frac{1}{N_{AV}} \frac{N_m}{\pi\left[R^2 - (a+\sigma_m)^2\right]H} \tag{6}$$

at that instant.

The energy change associated with the ionization of a group, μ_s, is represented as a function of pH in the aqueous solution,

$$\mu_s = \ln(10) k_B T (pK_0 - pH) \tag{7}$$

where pK_0 is the negative logarithm of the intrinsic dissociation constant of the group in the salt-free solution. The total energy with the ionization is expressed obviously as

$$U_s = N_m \mu_s \tag{8}$$

The definitions in eqs. (7) and (8) satisfy the consistency of the relations of the apparent dissociation constant to the pH and the degree of ionization.

As the interaction between all charged species in the cell (the ionized groups and dissociated counterions), a simple charged hard-sphere model, primitive model, is adopted here. The potential between two species, labeled as i and j, is defined as the Coulombic interaction with the hard core repulsion, as follows:

$$\phi_{i,j} = \begin{cases} \dfrac{1}{4\pi\epsilon_0 D} \dfrac{q_i q_j}{|r_i - r_j|} & |r_i - r_j| > \sigma_i + \sigma_j \\ \infty & |r_i - r_j| \leqslant \sigma_i + \sigma_j \end{cases} \tag{9}$$

where q, r and σ with subscript i or j denote the charge, the position and the radius of the each species, respectively. This naive assumption seems to be suitable for the primary examination. The cell space, including the inside of the polymer rod, is assumed to be a uniform dielectric continuum. Similar to the other MC works, the contribution of the electrostatic energy from the external cell is also considered in the calculations to eliminate the end effect of the system. The practical calculation of the electrostatic potential is almost the same as that of ref. [15], such as the minimum image (MI) energy with a pair of ions in the central cell and the self-consistent (SC) method for the external potential [15]. Then, the

total electrostatic energy, U_{el} is represented as follows,

$$U_{el} = N_p u_{el} = \sum_{\langle ij \rangle} \frac{1}{4\pi\epsilon_0 D} \frac{q_i q_j}{|r_i - r_j|_{MI}} + \sum_i q_i \Phi^L_{EXT}(r_i) \quad (10)$$

where the charge, q and its position, r are numbered consecutively by subscript i or j, and $\Phi^L_{EXT}(r_i)$ is the external potential at position, r_i, i.e. the contribution of the potential due to the charge distributions in external cells extending from $H/2$ to L. $|r_i - r_j|_{MI}$ is evaluated with the smallest difference in z coordinates among three possibilities: $|z_i - z_j|$, $|z_i - z_j \pm H|$. The total energy in the cell system is described by the sum of two quantities, U_s and U_{el}. These values are iteratively calculated in the loop to determine the acceptance of the MC trials. Several quantities are averaged by the summation of the values in the MC trial loop. The detailed descriptions of the MC trials are presented in the following sections.

At a known pH, negative logarithm of apparent dissociation constant, pK_a, is defined, as

$$pK_a = pH + \log[(1-\alpha)/\alpha] \quad (11)$$

where α denotes the averaged degree of ionization here. The instantaneous values in the MC loop and averaged ones, which are evaluated finally after all trial loop, are not distinguished in the notation of the present paper. By the thermodynamic consideration, the following expression is well known [22]:

$$pK_a = pK_0 + \frac{1}{\ln(10) k_B T} \frac{\partial g_{el}}{\partial \alpha} \quad (12)$$

where g_{el} is the electrostatic free energy of the system per one ionizable group as a function of α. Throughout this paper, thermodynamic quantities in lower-case letter denote the values per single ionizable group. The electrostatic term of pK_a, ΔpK, against α is denoted as the titration curve in the paper.

$$\Delta pK = pK_a - pK_0 = \frac{1}{\ln(10) k_B T} \frac{\partial g_{el}}{\partial \alpha} = pH + \log[(1-\alpha)/\alpha] - pK_0 \quad (13)$$

If the electrostatic interaction between the charged species can be neglected, this term must be constantly zero.

2.2. Algorithm for simulation and the details of calculation

In the iterative loop of the present MC simulation, one of three kinds of trials is taken for each pair of the ionizable group and counterion, such as ionization, deionization and movement of the counterion. All ionizable groups and counterions are numbered even if any counterions are deleted. The MC trials are carried out in order of the counterion number within single loop. The results are not affected even if the counterion is randomly chosen. The state of each counterion is checked before the beginning of the trial and the kind of the trial is determined in the following manner. If the counterion has been deleted from the cell by the deionization, the ionization trial of the pair of the counterion and the ionized group on the polymer rod is attempted with a definite probability, p, using pseudo-random number. If the counterion is really present in the cell, the deionization trial of the pair of the counterion and the ionized group is chosen with the same probability, p, and the random movement of the counterion is tried with the remaining probability, $1-p$. The acceptance of these trials is determined by Metropolis' algorithm using the probability function of the energy change of the system [23]. The results are independent of the probability p unless p is so low, e.g., below 0.2. When $p = 1$, the movement trials are not examined. Considering the efficiency and the accuracy of the computation, the probability, $p = 0.5$, is chosen in almost all cases. The details of each trial are described as follows:

(1) Ionization of un-ionized group

An ionization trial is composed of the charging up of un-ionized group on the polymer rod and the insertion of a counterion in the cell. The position of the insertion is determined using cylindrical coordinates with three random numbers to be uniformly distributed in the whole cell

volume, as follows:

$$r_i = R\sqrt{\rho_r}$$

$$\theta_i = 2\pi\rho_\theta$$

$$z_i = H\rho_H \qquad (14)$$

where r, θ and z with subscript i denote the radius, angle and height of the ith counterion, respectively. Each ρ with a subscript is a random number distributed uniformly within the range from 0 to 1. The combination of a counterion and an ionized group is already determined at the deionization process. The trial is obviously rejected if the collision occurs between the inserted counterion and the polymer rod or other counterions. Since two charged species are created in the cell, the change of the electrostatic energy with the ionization, ΔE_I, must be computed by the summation of the energy between the two charges and other charge species. Taking account of the excess energy with the ionization of a group, μ_s, the acceptance or the rejection of the trial is determined by Metropolis' criterion using the following probability function:

$$P_I = \min\{1, \exp[-(\Delta E_I + \mu_s)/k_B T]\} \qquad (15)$$

If the ionization trial is accepted, a new configuration is set instead of old one, such that the counterion is really inserted in the cell and the group is charged up.

(2) Deionization of ionized group

A deionization process is the combination of the deletion of a counterion from the cell and the un-ionization of a randomly chosen ionized group. The energy change with the pair charging off, ΔE_D, is calculated, and the acceptance is judged similarly to the above trials by the following probability,

$$P_D = \min\{1, \exp[-(\Delta E_D - \mu_s)/k_B T]\} \qquad (16)$$

If the deionization trial is accepted, the counterion becomes dimensionless having no charge and the ionized group is deionized, until the counterion is inserted by the ionization process again. The combination of the deleted counterion and the deionized group is kept until the next ionization.

(3) Movement of counterion

A counterion can be moved to a new trial position expressed by the Cartesian coordinates within a definite step width using uniform random numbers. The trial is rejected if the collision occurs with the polymer rod or other ions. The trial is also rejected if the ion moves away from the cylindrical cell. If the new axial position, z, is less than zero, it is replaced by $z + H$ and x and y are multiplied by -1. If z is greater than H, it is replaced by $z - H$ and x and y are multiplied by -1. The probability function of the acceptance is described as follows:

$$p_M = \min\{1, \exp(-\Delta E_M/k_B T)\} \qquad (17)$$

where ΔE_M is the energy change with the movement. The step width of the movement trial is regulated to give the acceptance ratio of the trial 0.5 in the early discarded loop. The results are not so affected by the ratio in the range around 0.5.

Contrary to the movement trial, the acceptance ratio of ionization and deionization trials is uncontrollable by any parameter, which causes a problem under the condition of high group density and high α range, as well as thinner radius of the polyion rod. The width of energy change with ionization–deionization trials often becomes too large to make a sufficient number of transitions under this condition. If the acceptance ratio, usually between 0.43 and 0.15, comes below the lower limit, the titration curves shift upward relatively to the estimation from the derivative of the free energy with α. In such cases, the obtained degree of ionization becomes somewhat doubtful, and hence the result is discarded by the empirical judgment.

Starting at a randomly chosen initial state, the MC trial iterations are controlled by the double loop (main loop and sub-loop). One cycle contains one Monte Carlo step (MCS) per counterion. A single sub-loop contains 250 cycles and 40 sub-loops are iterated in a main loop. In the standard simulation, the cell has 100 ionizable groups on the polymer rod. Therefore, 10^6 trials (10^4 MCS) are attempted in the single MC run at a given pH value. The convergence of the quantities is achieved in early stage (within about 1000 MCS; 10^5 trials). After 5000 discarded MCS, the

degree of ionization, the radial distribution of the mobile ions and other thermodynamic quantities are finally evaluated by summing up in the later 5000 MCS.

The cell with a radius of 100 Å and a height of 200 Å is chosen as the standard cell dimension. The cell height is so large that the external potential becomes ineffective. When N_p is 100, the axial distance per group is 2 Å, and its mean concentration, C_p, is 26.428 mmol/dm^3 (mM). In other cases the cell radius is in the range from 50 to 200 Å and the cell height is in the range from 50 to 400 Å. The total length of the combined cell system, the sum of the length of the central cell and two external cells on both sides, $2L$, is 10^4 Å. The radius of the polymer rod, a, and that of the counterion, σ_m, is determined so that the sum of two radii, which is the closest radius of the center of the counterion, is constantly 5 Å. The combination of the radius of the polymer rod and radius of the counterion is described as a (2 + 3) case if the polymer radius is 2 Å and the counterion radius is 3 Å, for example. The concentration of counterions in the cell free volume is 26.495 mmol/dm^3 (mM) at fully ionized state in the standard cell dimension, i.e. $H = 200$ Å, $R =$ 100 Å and $N_p = 100$.

The titration curve depends on the arrangement of the ionizable groups on the polymer rod surface. Various arrangements can be considered as the model polyelectrolytes. In the present study, two types of helical group arrangement are applied. The helix consists of four groups per turn and a mean translation along the helix is b. This leads to a pitch of $4b$. The first is an equidistant helical arrangement, helix A, as a reference case. The coordinates of the ith (from 1 to N_p) ionizable group are described as,

$$x_i = a\cos\left(\frac{\pi}{2}(i-1)\right)$$

$$y_i = a\sin\left(\frac{\pi}{2}(i-1)\right)$$

$$z_i = b(i-1) + 0.5b \qquad (18)$$

The second is a non-equidistant helix B, examined as an example of the irregular arrangement. The z component of the coordinate of helix A is modified as follows:

$$z_i = \begin{cases} b(i-1) + 0.75b & \text{if } i \text{ is odd} \\ b(i-2) + 1.25b & \text{if } i \text{ is even} \end{cases} \qquad (19)$$

where the ratio of the displacement of z component becomes 1:3. In that case, the mean axial distance per group is also b.

To measure the radial counterion distributions, the cell free volume is divided by the thin concentric shells whose width is in the range from 0.5 to 1.5 Å. The number of counterions in each shell is counted and summed up after the MC trial for each ion species, giving the radial concentration. Using the distributions, the entropy part of the mobile ion accumulation is calculated as described in the following section. The external potential is enumerated after each iterative sub-loop using the temporary concentration in the shells.

The numerical constants used in the simulation are $T = 298.15$ K and $D = 78.55$. Then, the Bjerrum length, l_B,

$$l_B = e^2/(4\pi\epsilon_0 D k_B T) \qquad (20)$$

is taken as 7.135 Å. The maximum charge density parameter on the polyion rod, ξ^{max}, is 3.5675, when b is 2 Å. The uniform pseudo-random numbers are generated by the well-examined shift register method, and used after a short warming-up [24–26]. Almost all MC simulations are executed on the vector processor (FACOM VP-200 and VP-2600) in the computational center of Nagoya University.

2.3. Estimation of the electrostatic free energy

In the MC simulation, the contribution of the free energy from the electrostatic interaction is evaluated by two distinctive manners. The first is the integration of the resultant titration curve using a conventional fitting function. The second is the estimation of each part of the electrostatic free energy. In the second way, the entropy part is the central theme. The detailed procedures are described as follows:

(1) Numerical integration of the titration curve

The titration curve is fitted by a suitable func-

tion; for example, a third-order or fourth-order polynomial without zeroth-order term, and g_{el} is represented by the integral form of this function using the relation of eq. (13). The results are not affected by the selection of the function, whenever the fitting is satisfactory.

(2) Measurement of the entropy in the system

According to the thermodynamic consideration, the free energy of the system per single ionizable group is composed of three terms, as follows:

$$g_{el} = u_{el} - (s_{el,p} + s_{el,m})T \tag{21}$$

where u_{el} is the enthalpy of the electrostatic interaction, $s_{el,m}$ is the contribution of the entropy of the counterion accumulation, and $s_{el,p}$ is that of the mixing of the state of ionizable groups. The third term appears only in the discrete site model [10]. The term u_{el} is represented in eq. (10), and $s_{el,m}$ is estimated from the counterion radial distribution as

$$S_{el,m} = N_p s_{el,m} - N_{AV} k_B \int_v C_m \ln(C_m/C_m^{mean})\, dv \approx -N_{AV} k_B 2\pi \Delta r H \sum_k r_k C_{m,k} \ln(C_{m,k}/C_m^{mean}) \tag{22}$$

where k is the serial number of the shell, r_k, the radius of the middle point of the kth shell; Δr, its width, and $C_{m,k}$, the counterion concentration in the shell [27]. The diversities of the longitudinal and angular distributions, which do not seem to be significant, are neglected in the calculation. In addition, the effect of the core potential (the excluded volume) and the repulsion between the released counterions is not considered.

The value of $s_{el,p}$ is calculated as the difference in the total entropy, $s_{tot,p}$ and the entropy of random mixing, $s_{rand,p}$, as follows:

$$S_{el,p} = N_p s_{el,p} = N_p(s_{tot,p} - s_{rand,p}) \tag{23}$$

The total entropy is evaluated from the probabilities of the ionization patterns and the entropy of random mixing is defined by the averaged degree of ionization, as follows:

$$N_p s_{tot,p} = -k_B \sum_l p_l \ln(p_l)$$

$$N_p s_{rand,p} = -N_p k_B[\alpha \ln\alpha + (1-\alpha)\ln(1-\alpha)] \tag{24}$$

where p_l is the probability taking the lth ionization pattern in the helically arranged lattice of the ionizable groups. In practical calculation, several thousand states of central 10 groups are used as the samples to evaluate the set of the probability, p_l.

2.4. Computation at a fixed degree of ionization

The procedure of the Monte Carlo simulation for the polyelectrolyte at a fixed degree of ionization is almost the same as the process above without ionization–deionization trial. The movement trials of the counterions are only iterated around a partially ionized polyion with a helical group arrangement above described using a probability function, eq. (17). The counterion distribution as well as the thermodynamic quantities is evaluated at a given α in a similar manner.

2.5. Solution of the Poisson–Boltzmann equation

The Poisson–Boltzmann equation was analytically solved for an infinitely long rod-like polyelectrolyte with counterions in a cylindrical coordinate [28,29]. The electrostatic energy and the electrostatic free energy were also evaluated analytically from the solution [30].

To calculate the apparent dissociation constant, the following relation is applicable:

$$\frac{\partial g_{el}}{\partial \alpha} = -e\psi(a) \tag{25}$$

where $\psi(a)$ is the surface potential on the polymer rod, which is set to zero at the point where the local counterion concentration is equal to the mean counterion concentration in the cell [31]. If the counterion has a finite radius, σ_m, the surface potential is given by the following equation:

$$\psi(a) = \psi(a+\sigma_m) + \frac{-e\alpha}{2\pi\epsilon_0 Db} \ln\left(\frac{a+\sigma_m}{a}\right) \tag{26}$$

where $\psi(a+\sigma_m)$ is the potential at the closest radius of the center of counterion, which is analytically evaluated by the PB equation [32,33]. The values of ΔpK are evaluated numerically using eq. (13) based on these relationships.

3. Results

3.1. Radial distribution of the counterions

At first, the results of the simulation on the counterion distributions are presented. Around the fully ionized polyion at $\xi = 3.5675$, the movement trial of the mobile ion is only examined in the MC trial loop. The radial distributions are shown for the three different combinations of the radius of the polymer rod and the counterion with the analytical results of the PB equation in Fig. 1. The overall distribution profiles resemble the results of the PB equation as shown in Fig. 1a. The expanded figure, Fig. 1b, is drawn to clarify the difference between the MC results and the PB solutions. In the case of a (2 + 3) radius combination (the polymer radius is 2 Å and the counterion radius is 3 Å), the agreement between them is excellent. In the (3 + 2) case, the concentrations of the counterion near the polyion are higher than the analytical PB solutions, and the values far from the rod are lower than those of the PB result. In the (1 + 4) case, the opposite tendency appears. The concentrations near the polyion are lower and those far from the rod are higher than the PB result. Furthermore, a slight shoulder appears in this case. This shoulder becomes more apparent in the case of higher charge density. The counterion concentrations in three cases become indistinguishable near the outer boundary of the cell. Similar results have already been presented in the MC works [14]. These results mean that the electrostatic field attracts the counterions toward the polyion more strongly than the case of the PB equation, whereas the excluded volume effect of the counterion prevents others from approaching the polyion. Both effects, not expected in the PB equation, may cancel each other in the (2 + 3) case. These characteristics are almost independent of the arrangement of the charged groups on the polymer rod.

3.2. Simulated titration curves with the PB solutions

At different pH, the MC simulation is carried out with ionization–deionization trials as well as the counterion movements. The averaged degree of ionization and other quantities are obtained

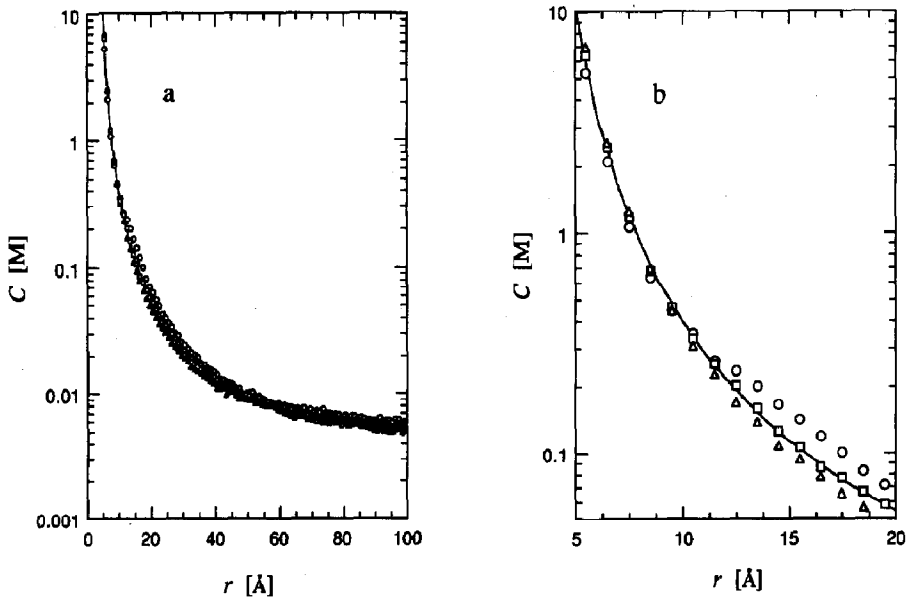

Fig. 1. Radial distribution of counterions around the polyion rod at fully charged state, $\xi = 3.5675$ ($b = 2$ Å) by the MC simulations in the standard cell dimension (see text) for the three different combinations of the radius of polyion rod and counterion. (○) (1 + 4) case, (□) (2 + 3) case, and (△) (3 + 2) case. The arrangement of the charge on the polyion is equidistant along its helix axis, helix A. The solution of the PB equation is presented by solid line. (a) overall profile and (b) extended view.

with sufficient accuracy under the standard conditions. The titration curves evaluated with eq. (11) are presented in three cases of the radius combination in Fig. 2. In the figure, the analytical solutions of the PB method are also shown by the smooth lines in the five cases of the radius combination. In each case of the radius combination, an appreciable difference in the curve is observed between the MC simulation and the PB result. Each ΔpK value by the MC method is so lower than the PB calculation at any degree of ionization. To fit the PB solution to the MC result, a thicker radius of the polymer is necessary. These differences are also observed in other cases of various concentrations of the polyion and various densities of the groups on the polymer.

The deviation of the titration curve must be explained by the difference in the electrostatic free energy between both systems. The difference, however, is not clearly observed on the counterion radial distribution. In Fig. 3, the counterion distributions are represented in the (2 + 3) case at three values of α (about 0.2, 0.45, and 0.8). The agreement between the MC simulation and the PB result is satisfactory in each degree of ionization. This indicates that the entropy of the counterion distribution is well predicted by the PB equation in that case. In other cases of the radius combination, the agreement of the distribution between both systems becomes a little poorer, and the tendencies of the deviation are the same as those described in section 3.1.

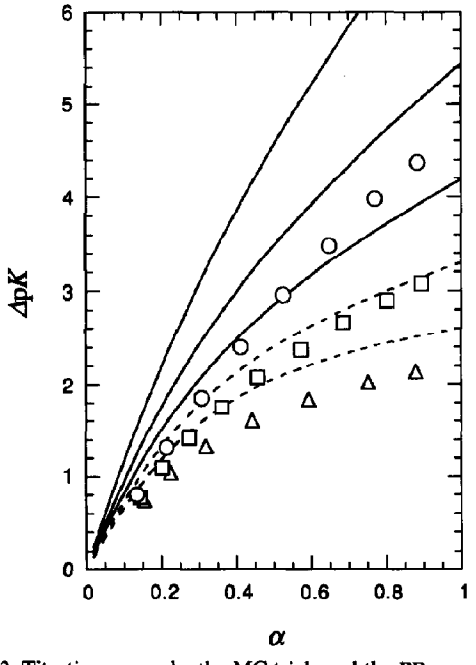

Fig. 2. Titration curves by the MC trials and the PB equations for several different radius combinations in salt-free systems. The cell dimension is the same as the standard case (see text) and $b = 2$ Å ($\xi^{max} = 3.5675$). The arrangement of the ionizable groups is the helix A. The results of the MC simulation are represented by symbols. (○) (1+4) case, (□) (2+3) case, and (△) (3+2) case. The solutions of the PB equation are represented by lines. Solid lines: (1+4) case, (2+3) case, and (3+2) case, broken lines: (4+1) case and (5+0) case, from top to bottom.

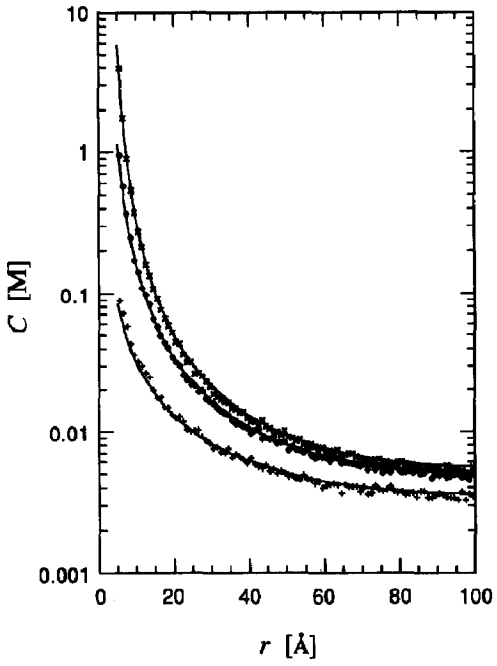

Fig. 3. Comparison of the counterion distributions by the MC simulations (symbols) of the potentiometric titration with the PB solutions (lines) at three different degrees of ionization in the case of (2+3) radius combination presented in Fig. 2. (×) $\alpha = 0.798258$, (◇) $\alpha = 0.454248$, and (+) $\alpha = 0.203316$, from top to bottom.

3.3. Electrostatic free energy

In Fig. 4, the electrostatic parts of the free energy by the MC works are shown with the PB solutions. At first, it must be emphasized that the agreement of the free energies estimated by the

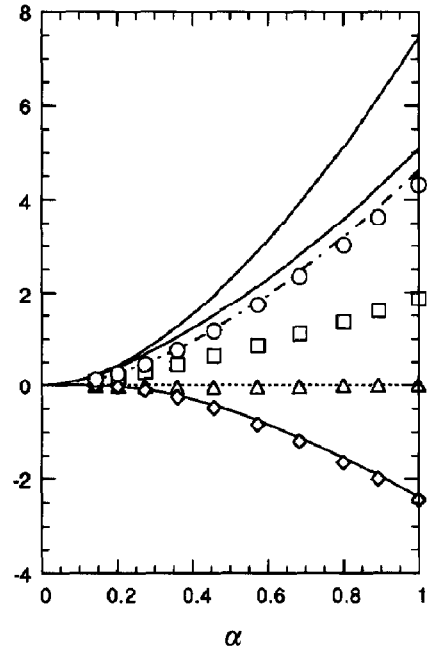

Fig. 4. Electrostatic contributions of the free energy as function of α in the case of (2+3) radius combination in Fig. 2. The MC results evaluated by the second manner (see text) are represented by symbols, (□) u_{el}/k_BT, (◇) $s_{el,m}/k_B$, (△) $s_{el,p}/k_B$, and (○) g_{el}/k_BT. In the figure, the thermodynamic quantities are plotted as the reduced values divided by the k_BT or k_B. The values at $\alpha = 1$ are obtained by the MC simulation of the counterion distribution at fully ionized state, where $s_{el,p}/k_B$ must to be zero. Chain line represents g_{el}/k_BT by the integration of the titration curve (the first manner). Solid lines represent the PB solutions, g_{el}/k_BT, u_{el}/k_BT, and $s_{el,m}/k_B$ from top to bottom. Dotted line is a base line.

two distinctive manners in the MC method is very good. The agreement between the integration of the titration curve (chain line) and the result by the estimation of the each part of the free energy (open circle) is satisfactory in this condition. This fact indicates the consistency of the present MC simulation. However, a slight deviation is observed in high α range and the agreement becomes poorer in the case of the higher charge density. This deviation is due to the problem of the large energy gap in the titration simulation and/or the inaccuracy of the entropy of the counterion accumulation. It seems that the effect of the repulsion between the counterions on the entropy term appears significantly at high charge density cases.

Comparing the part of the electrostatic free energy of the MC calculations with those of the PB solutions, the entropy part by the counterion accumulation is close between both results as suggested by the agreement of the counterion distributions. In the case of other radius combination, the entropy values are not different from those in this case. The large difference in the free energy is mostly induced by the enthalpy part, such that the difference in the electrostatic energy makes this deviation. This seems to be caused by the difference in the charge distribution between both systems and the hypothesis in the PB equation, as discussed later.

The values at the $\alpha = 1$ in Fig. 4 are obtained by the simulation at the fully ionized state, instead of allowing the distribution of α. The energy values calculated at the other fixed α agree with those in this figure except for the entropy of the state of ionizable groups (data not shown).

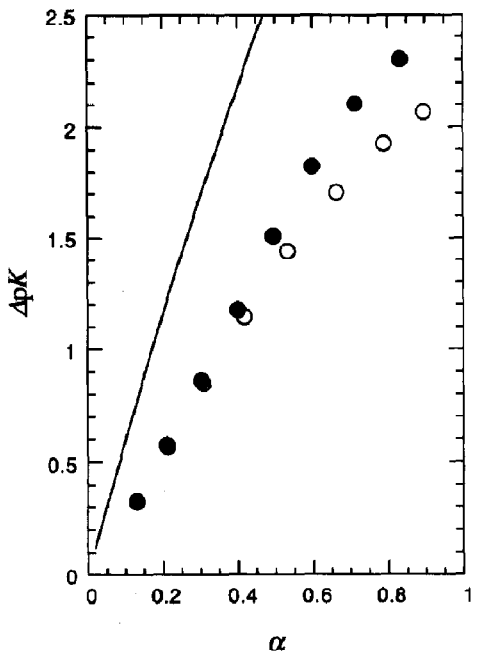

Fig. 5. Titration curves for two helical arrangements of the ionized groups of the polymer rod surface in the (1+4) radius combination case. The rod with 100 ionizable groups is assumed in the cell with a radius of 100 Å and a height of 400 Å. Thus, the mean axial distance per group, $b = 4$ Å ($\xi^{max} = 1.78375$). Open circle: helix A, closed circle: helix B, and line: PB result.

This indicates that the distribution of α is too narrow to affect the thermodynamic quantities in the titration simulation. Indeed, the width of the distribution of α, $\Delta\alpha$, is below 0.04 in almost all cases examined.

3.4. Dependence on the arrangement of the polyion charge

To investigate the effect of the difference in the group arrangement on the polymer rod surface, the titration profile of helix A is compared with that of helix B in the (1 + 4) case at $b = 4$ Å ($\xi^{max} = 1.78375$), shown in Fig. 5. In the low ionization range ($\alpha \leqslant 0.3$), the values of ΔpK are found to agree well in both cases. A slight jump of the titration curve appears with helix B around $\alpha = 0.5$, due to the difference in the steepness of the curvature of the electrostatic free energy. Indeed, the free energy of helix B increases more steeply than that of helix A around $\alpha = 0.5$ as shown in Fig. 6. Apparent distinction, however, is not detected on the counterion distribution and the entropy by the counterion accumulation between both helices. The source of the jump in the case of helix B is ascribed to the difference in the electrostatic energy between the polyion charges. The alternating ionization may be more favorable in the middle α range in the helix B, as indicated in the entropy of the mixing of the ionized state, $s_{el,p}$, in which the deeper valley appeared in the helix B (Fig. 6). However, this entropy term is so small that the free energy of the system is not affected by the deviation of the entropy. The effect of the arrangement becomes smaller for the thicker rod because of the spatial longer distance between the charged group on the polymer surface. Indeed, the difference is not observed between both helical arrangements in the case of (3 + 2) radius combination.

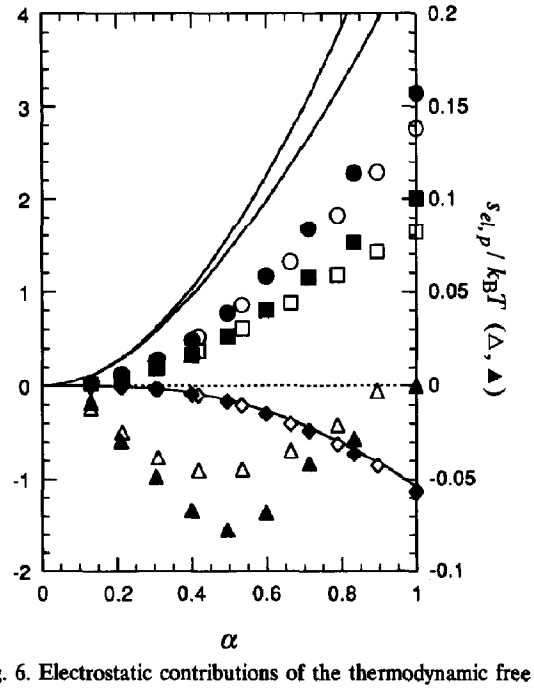

Fig. 6. Electrostatic contributions of the thermodynamic free energy for two helical arrangements of the ionized groups. Other details are the same as in Fig. 5. The symbols and lines are the same as in Fig. 4. Open symbol: helix A and closed symbol: helix B. $s_{el,p}/k_B$ by the MC simulation is expanded with the right axis.

4. Discussion

4.1. Characteristics of the present MC simulations

It becomes possible to simulate the potentiometric titration behavior for the rod-like polyelectrolyte in solution by incorporating not only the movement of the small ion but also the ionization–deionization of the ionizable groups. The correlation between the states of the ionizable groups are clearly demonstrated by taking into account the ionization–deionization process. The degree of ionization as well as the small ion distribution is evaluated at the same time at a given pH by this new MC method. The averaged values thus obtained are the ensemble averages of the polymers with the different degree of ionization. The consideration of the distribution of α is an advanced point of the present MC simulation method, contrary to the previous works which have treated the state at a fixed α. This method is valuable for the more detailed investigations on the spacial behavior or the local processes of the ionizable group and of the mobile ion. Nevertheless, the distribution of the degree of ionization is so limited that its influence on the titration profile is not remarkable in the present study. It

seems that the quantities are not so different from those in the case of the fixed degree of ionization.

The calculation of the electrostatic energy becomes possible by applying the discrete site model as the polyion charge distribution. The entropy of the counterion distribution can also be estimated using its radial distribution. Furthermore, the entropy of the mixing state of the ionizable groups is evaluated, though the effect is inconsiderable. The whole electrostatic free energy in the system can be analyzed by these calculations. The dependence of the group arrangement on the titration behavior can be examined by this model. This is another characteristic point of the present study.

The only difficulty of the method appears in the cases at the higher charge density of the thinner polyion rod, where the transition probability of the ionization–deionization trial becomes too low to generate the equilibrium state sufficiently. This is a common problem in the MC simulation of the complicated system.

Considering the above points, an alternative method can be applied to simulate the potentiometric titration by calculating the electrostatic free energies. The free energies are evaluated at various fixed degrees of ionization and its curve against α is fitted by a suitable function. The titration curve is obtained by differentiation of the fitting curve with the degree of ionization based on eq. (13). This method must be effective in the cases where the direct simulation of the ionization–deionization is difficult because of the low transition probability. To calculate the electrostatic free energy accurately, the effect of mixing of the ionized states must be considered. In addition, more detailed considerations are required for the entropy of the small ion distribution by taking account of the repulsion effect.

4.2. Comparison of the present MC system with the PB equation

The large deviation is observed on the titration curve by this MC simulation from the solution of the PB equation. It is found that this deviation is due to the difference in the electrostatic energy term by analyzing the contributions of the free energy. The entropy terms by the counterion accumulation coincide relatively well between both systems, and the entropy of the mixing of the ionized state of the ionizable groups is inconsiderable.

There are two different points between the present MC system and the PB system. One is the difference in the distribution of the polyion charge on the polymer, i.e. discrete distribution of the point charges and uniformly smeared charge distribution. Another is the approximation for the charge and potential adopted in the PB equation.

The calculation procedure of the electrostatic energy is different between both systems due to the difference in the charge distribution. This is one reason of the deviation of the electrostatic energy between both systems. In the discrete charge system, the pair interaction of the individual point charges is only considered. In the summation of these terms, the self-energy of the point charge is missing, contrary to the system of the uniform charge distribution. In the MC system, the effect of the arrangement of the ionizable groups mainly appears in the electrostatic repulsion between the ionized groups on the polymer. This term is determined by the three-dimensional distance between the nearer groups. Therefore, the various titration curves are obtained depending on its arrangement even if the mean linear density and the radius combination are the same.

The approximation of the PB equation seems to be another source of the energy deviation. In the PB hypothesis, the counterion charge is assumed to be continuously distributed in the cell free volume. The correlation among the ionic species and the excluded volume effect of the counterions are ignored [14,34]. Indeed, there is a slight deviation of the electrostatic potential of the MC simulation from the PB solution (data not shown). From this deviation, a slight difference arises in the counterion distribution between both systems depending on the combination of the radius of the polymer rod and the counterion. This must be ascribed to the approximation in the PB equation itself.

Above two differences reduce the electrostatic energy term of the MC system in comparison with

that of the PB system. It is difficult to divide two contributions to the deviation quantitatively because the position where the electrostatic potential is equal to zero cannot exactly correspond between two systems. The investigation on the effect of the valency of counterions will be valuable for the further studies to clarify this respect. However, the result of the MC study must be also suggestive to other studies on the electrolyte system.

In the present stage, the comparison of the simulation with the experimental data is not tried because the proper experiment is not present on the rod-like polyelectrolyte over a wide range of α in the salt-free solution. The application to the system of added salt case must be examined as a further study. However, a suggestion is obtained about the difference of the experimental data with the PB solution. Though the difference between the experimental data and the PB results have been previously discussed by some secondary factors, such as the dielectric constant of the medium and/or the ion hydration, the essential problem seems to be the approximation of the uniformly charged model and the PB equation [4]. The real polyelectrolyte system consists of the point charges.

4.3. Further refinement and other remarks

Various points on the theoretical prediction of the polyelectrolyte titration behavior have been exhibited by the author [10]. Some of them will be able to overcome by this MC simulation for the rod-like polyelectrolytes in principle.

The effects of the distance dependence of the dielectric constant and the ion hydration are studied with various models [35–37]. In the present study, the primitive model is adopted as the ionic interaction. These effects will be resolved phenomenologically by the refinement of the interaction potential. A more realistic model is required for the interpretation of the experimental results.

In the case of the flexible polyion, the chain expansion with the increase in degree of ionization is extensively studied [38,39]. Recently the titration behavior of the flexible polyelectrolytes is simulated by the MC method by taking into account the polymer chain expansions [40,41]. Nevertheless the interaction between the polyion charges is simplified by adopting the DH type screened Coulombic potential in most studies.

There is an important remaining problem, however, overlooked in the previous polyelectrolyte theories. It is on the ionization of water related to the our treatment of pH. In this study, the solution pH is assumed as a fixed parameter of the field that determines the energy with the transition of the ionizable group, represented in eqs. (7) and (8). Thus the effect of the distribution of the charged ionized water molecules (H_3O^+ and OH^-) and those fluctuations are ignored. This situation is similar to the PB method that determines the free energy at a fixed degree of ionization where the ionized water species are considered to be negligible. This consideration is appropriate in the case of neutral pH solution, but at the low or high pH, the effect of the ionized water species must be examined. Fluctuations of the polyion charges actually occur under a constant number of counterions due to the dissociation equilibrium between H^+ and the ionized group. The behavior of the ionized water may be different from that of other ionic species [14]. The increase of the counterion activity in the polymer solution of maleic acid in high α range will be explained by the difference of the behavior of the proton from that of the metal counterion [42]. The concentration of H^+ near the DNA molecule is obtained with the PB equation [43]. Explicit treatment of the ionized water molecules is required for the complete understanding of the aqueous polyelectrolyte solutions. The progress of the present simulation method is necessary for this purpose.

5. Acknowledgement

The author is grateful to Professor Akira Minakata for valuable suggestions and critical reading of the manuscript, and to Mr. Nozue and Ms. Sugaya for helpful support.

6. References

[1] L. Kotin and M. Nagasawa, J. Chem. Phys. 36 (1962) 873.
[2] M. Nagasawa, Pure Appl. Chem. 26 (1971) 519.
[3] Y. Muroga, K. Suzuki, Y. Kawaguchi and M. Nagasawa, Biopolymers 11 (1972) 137.
[4] S. Sugai and K. Nitta, Biopolymers 12 (1973) 1363.
[5] G.S. Manning, J. Phys. Chem. 85 (1981) 870.
[6] S. Lifson, J. Chem. Phys. 26 (1957) 727.
[7] A. Minakata, K. Matsumura, S. Sasaki and H. Ohnuma, Macromolecules 13 (1980) 1549.
[8] S. Sasaki and A. Minakata, Biophys. Chem. 11 (1980) 199.
[9] R.L. Cleland, Macromolecules 17 (1984) 634.
[10] T. Nishio, Biophys. Chem. 40 (1991) 19.
[11] T. Nishio, Rep. Progr. Polymer Phys. Japan 34 (1991) 47.
[12] S. Kawaguchi, T. Kitano, K. Ito and A. Minakata, Macromolecules 23 (1990) 731.
[13] K. Binder, ed., Monte Carlo methods in statistical physics (Springer, Berlin, 1986).
[14] M. Le Bret and B.H. Zimm, Biopolymers 23 (1984) 271.
[15] P. Mills, C.F. Anderson and M.T. Record Jr., J. Phys. Chem. 89 (1985) 3984.
[16] P. Mills, C.F. Anderson and M.T. Record Jr., J. Phys. Chem. 90 (1986) 6541.
[17] C.S. Murthy, R.J. Bacquet and P.J. Rossky, J. Phys. Chem. 89 (1985) 701.
[18] V. Vlachy and A.D.J. Haymet, J. Chem. Phys. 84 (1986) 5874.
[19] C.F. Anderson and M.T. Record Jr., Annu. Rev. Biophys. Biophys. Chem. 19 (1990) 423.
[20] B. Jayaram, S. Swaminathan, D.L. Beveridge, K. Sharp and B. Honig, Macromolecules 23 (1990) 3156.
[21] B. Jayaram and D.L. Beveridge, J. Phys. Chem. 95 (1991) 2506.
[22] A. Katchalsky and J. Gillis, Rec. trav. chim. 68 (1949) 879.
[23] N. Metropolis, A.W. Rosenbluth, M.N. Rosenbluth, A.H. Teller and E. Teller, J. Chem. Phys. 21 (1953) 1087.
[24] R.C. Tausworthe, Math. Comput. 19 (1965) 201.
[25] S. Kirkpatrick and E.P. Stoll, J. Comput. Phys. 40 (1981) 517.
[26] N. Ito and Y. Kanada, Supercomputer 7 (1990) 29.
[27] F. Oosawa, Polyelectrolytes (Marcel Dekker, New York, 1971).
[28] T. Alfrey Jr., P.W. Berg and H. Morawetz, J. Polym. Sci. 7 (1951) 543.
[29] R.M. Fuoss, A. Katchalsky and S. Lifson, Proc. Natl. Acad. Sci. USA 37 (1951) 579.
[30] S. Lifson and A. Katchalsky, J. Polym. Sci. 13 (1954) 43.
[31] K.A. Sharp and B. Honig, J. Phys. Chem. 94 (1990) 7684.
[32] T.L. Hill, Arch. Biochem. Biophys. 57 (1955) 229.
[33] M. Le Bret and B.H. Zimm, Biopolymers 23 (1984) 287.
[34] M. Fixman, J. Chem. Phys. 70 (1979) 4995.
[35] S. Takashima, A. Casaleggio, F. Giuliano, M. Morando, P. Arrigo and S. Ridella, Biophys. J. 49 (1986) 1003.
[36] M. Troll, D. Roitman, J. Conrad and B.H. Zimm, Macromolecules 19 (1986) 1186.
[37] J. Mazur and R.L. Jernigan, Biopolymers 31 (1991) 1615.
[38] G.A. Christos and S.L. Carnie, J. Chem. Phys. 92 (1990) 7661.
[39] H.H. Hooper, H.W. Blanch and J.M. Prausnitz, Macromolecules 23 (1990) 4820.
[40] C.E. Reed and W.F. Reed, J. Chem. Phys. 96 (1992) 1609.
[41] A.P. Sassi, S. Beltrán, H.H. Hooper, H.W. Blanch, J. Prausnitz and R.A. Siegel, J. Chem. Phys. 97 (1992) 8767.
[42] S. Kawaguchi, T. Kitano, K. Ito and A. Minakata, Macromolecules 24 (1991) 6335.
[43] G. Lamm and G.R. Pack, Proc. Natl. Acad. Sci. USA 87 (1990) 9033.